A Group A *Streptococcus* ADP-Ribosyltransferase Toxin Stimulates a Protective Interleukin 1β-Dependent Macrophage Immune Response

Ann E. Lin,[a] Federico C. Beasley,[a] Nadia Keller,[a] Andrew Hollands,[a] Rodolfo Urbano,[a] Emily R. Troemel,[b] Hal M. Hoffman,[a,c,e] Victor Nizet[a,d,e]

Department of Pediatrics,[a] Division of Biological Sciences,[b] Department of Medicine,[c] and Skaggs School of Pharmacy and Pharmaceutical Sciences,[d] University of California, San Diego, La Jolla, California, USA; Rady Children's Hospital, San Diego, CA, USA[e]

ABSTRACT   The M1T1 clone of group A *Streptococcus* (GAS) is associated with severe invasive infections, including necrotizing fasciitis and septicemia. During invasive M1T1 GAS disease, mutations in the *covRS* regulatory system led to upregulation of an ADP-ribosyltransferase, SpyA. Surprisingly, a GAS Δ*spyA* mutant was resistant to killing by macrophages and caused higher mortality with impaired bacterial clearance in a mouse intravenous challenge model. GAS expression of SpyA triggered macrophage cell death in association with caspase-1-dependent interleukin 1β (IL-1β) production, and differences between wild-type (WT) and Δ*spyA* GAS macrophage survival levels were lost in cells lacking caspase-1, NOD-like receptor protein 3 (NLRP3), apoptosis-associated speck-like protein (ASC), or pro-IL-1β. Similar *in vitro* findings were identified in macrophage studies performed with pseudomonal exotoxin A, another ADP-ribosylating toxin. Thus, SpyA triggers caspase-1-dependent inflammatory cell death in macrophages, revealing a toxin-triggered IL-1β-dependent innate immune response pathway critical in defense against invasive bacterial infection.

IMPORTANCE   Group A *Streptococcus* (GAS) is a leading human pathogen capable of producing invasive infections even in healthy individuals. GAS bacteria produce a toxin called SpyA that modifies host proteins through a process called ADP ribosylation. We describe how macrophages, frontline defenders of the host innate immune system, respond to SpyA by undergoing a specialized form of cell death in which they are activated to release the proinflammatory cytokine molecule interleukin 1β (IL-1β). Release of IL-1β activates host immune cell clearance of GAS, as we demonstrated in tissue culture models of macrophage bacterial killing and *in vivo* mouse infectious-challenge experiments. Similar macrophage responses to a related toxin of *Pseudomonas* bacteria were also shown. Thus, macrophages recognize certain bacterial toxins to activate a protective immune response in the host.

Address correspondence to Victor Nizet, vnizet@ucsd.edu.

*S*treptococcus pyogenes (group A *Streptococcus* [GAS]) is a leading bacterial pathogen responsible for a broad array of human diseases, ranging from superficial infections such as pharyngitis ("strep throat") to potentially life-threatening systemic conditions, including necrotizing fasciitis and streptococcal toxic shock syndrome (1). Spontaneous mutations in the *covRS* (also called *csrRS*) two-component regulatory system arise during systemic dissemination of the M1T1 GAS clone, which has spread globally in recent decades as the leading strain associated with severe infections (2). With *covRS* mutation, transcription of several genes encoding GAS hyaluronic acid biosynthesis, cytotoxins, and immune evasion factors is upregulated, promoting neutrophil resistance and bloodstream survival and thereby increasing virulence (3, 4). Hyperinvasive *covRS* derivatives are selected upon experimental challenge of mice with strain M1T1 (3, 5, 6) and other serotype GAS strains (7) and can be designated "animal-passaged" (AP) strains.

One gene that is highly upregulated upon *covRS* mutation in M1T1 GAS is *spyA*, encoding a membrane-bound C3-like ADP-ribosyltransferase capable of catalyzing the covalent transfer of an ADP ribose moiety of NAD$^+$ to target proteins (8–10). Several ADP-ribosyltransferase toxins of pathogenic bacteria, including *Pseudomonas* exotoxin A, cholera toxin, and diphtheria toxin, are associated with host cell death (reviewed in reference 11). Although SpyA can modify multiple cytoskeletal proteins in epithelial cells (12) and weakly contributes to lesion development in a mouse subcutaneous infection model (10), the effect of high-level SpyA expression following *covRS* mutation on invasive GAS bloodstream infection has not been studied.

Innate immune responses orchestrated by macrophages play key roles in defense against microbial infection. A form of morphologically and mechanistically distinct proinflammatory programmed macrophage cell death called "pyroptosis" has recently received attention as a mechanism stimulating pathogen clearance (13, 14). Unlike apoptosis, which is activated by a subset of caspases, including caspase-3, the key regulator inducing pyroptosis is caspase-1 (15). While apoptosis is an "immunologically silent" process marked by formation of membrane-bound apo-

ptotic bodies featuring cytoplasmic and nuclear condensation (13, 16), pyroptosis is a proinflammatory process characterized by rapid plasma membrane rupture and release of proinflammatory and immune-boosting cytokines interleukin 1β (IL-1β) and IL-18 (16, 17).

IL-1β has a key role in mediating effective macrophage host defense, promoting upregulation of antimicrobial molecules such as the proinflammatory cytokines tumor necrosis alpha (TNF-α) and IL-6 (18–20). Although several mechanisms have been proposed for IL-1β activation, the best studied involves protease caspase-1, which cleaves the inactive pro-IL-1β precursor to its mature form. Caspase-1 activity is predominantly regulated by inflammasomes—multimeric complexes comprised of caspase-1, various cytoplasmic pattern recognition receptors, such as NOD-like receptor protein 3 (NLRP3), and an adaptor protein called apoptosis-associated speck-like protein (ASC) (16, 21). Inflammasome responses restrict intracellular replication of numerous pathogens (13, 14, 16, 17), and failure to activate inflammasome oligomerization during microbial infections upon loss of a key inflammasome component(s) severely dampens macrophage killing, allowing accelerated bacterial replication (22, 23). Inflammasome- and caspase-1-dependent macrophage cell death is triggered in the presence of "danger signals" from intracellular pathogens such as *Shigella*, *Yersinia*, *Salmonella*, *Legionella*, and *Francisella* spp. (14–17). GAS pore-forming cytolysin streptolysin O (SLO) induces NLRP3 inflammasome-dependent signaling to activate caspase-1 and IL-1β secretion in macrophages (24), but the impact of this proinflammatory cell death on bacterial clearance and disease pathogenesis has not been analyzed.

Here we report that GAS SpyA initiates caspase-1-dependent signaling to induce IL-1β release. Proinflammatory macrophage cell death triggered in response to SpyA dramatically enhances clearance of bacteria and restricts bacterial growth, attenuating disease progression. Mice infected with an isogenic M1T1 GAS $\Delta spyA$ mutant experience significantly higher bacterial loads and mortality than animals infected with the wild-type (WT) parent strain. The importance of the IL-1β-dependent innate immune response to GAS was reemphasized in challenge studies of mice with impaired IL-1β signaling, which experienced higher bacterial burdens and mortality. Further, *Pseudomonas aeruginosa* C3-ADP ribosyl-transferase exotoxin A activates caspase-1-mediated IL-1β signaling to promote effective bacterial clearance, suggesting that host sensing of this family of toxins by macrophages initiates an IL-1β-dependent innate defense program.

RESULTS

SpyA is highly expressed in a hyperinvasive animal-passaged M1T1 GAS strain. A global microarray-based genetic screen suggested that *spyA* is highly upregulated in a hyperinvasive animal-passaged (AP) GAS M1T1 strain with mutations in the *covS* regulatory locus (3). In our well-characterized M1T1 GAS human invasive disease isolate (strain 5448) (25), real-time quantitative PCR (qPCR) results corroborated a 10-fold increase in *spyA* mRNA levels upon animal passage (see Fig. S1A in the supplemental material). To study the function of SpyA in GAS invasive-disease pathogenesis, we generated an isogenic in-frame allelic exchange $\Delta spyA$ knockout in the M1T1 AP background and complemented this mutant with the *spyA* gene on an expression plasmid (pSpyA). Successful deletion and complementation of *spyA*/

pSpyA were confirmed by real-time qPCR and Western blot analysis of a membrane protein preparation (see Fig. S1B and C).

SpyA-deficient GAS bacteria evade macrophage killing. A previous report suggested that SpyA influenced early innate immune signaling (10), leading us to investigate whether it could be manipulating the host immune response coordinated by macrophages. We infected murine bone marrow-derived macrophages (BMDMs) with WT or $\Delta spyA$ GAS for 2 and 4 h before lysing cells for bacterial recovery (total killing). While no difference was observed within 1 h of infection, we found the $\Delta spyA$ mutant was significantly less susceptible to macrophage killing than the WT strain at 2 h and at 4 h postinfection (Fig. 1A). By complementing the $\Delta spyA$ mutant in *trans* with *spyA* expressed on a plasmid vector (pSpyA), we restored the killing effect to WT levels, with reduced bacterial recovery from BMDMs (Fig. 1A). Similar results were found in J774 murine macrophages (see Fig. S2A in the supplemental material).

We continued to explore whether loss of SpyA also influences the level of phagocytosis and intracellular survival in macrophages. Using antibiotic protection to quantify intracellular CFU at different time points, increased levels of $\Delta spyA$ were seen at the earliest time point, consistent with the increased bacterial uptake described by Hoff et al. (10), while levels of intracellular survival of the WT and mutant bacteria were roughly equal over the ensuing 4 h (Fig. 1B). Since bacterial replication within murine BMDMs can sometimes be inefficient, we examined intracellular replication in murine macrophage cell line J774. There we found a difference between $\Delta spyA$ and WT GAS intracellular growth levels, as the $\Delta spyA$ strain replicated much more rapidly than the WT strain from 2 h to 4 h (see Fig. S2B in the supplemental material).

To further evaluate whether SpyA influences bacterial killing by macrophages by the use of gain-of-function analyses, we used *Staphylococcus aureus* RN4220 as a heterologous host to express SpyA (see Fig. S3A in the supplemental material). Intracellular bacterial survival was diminished in BMDMs infected with *S. aureus* pSpyA (Fig. 1C), indicating that SpyA triggers macrophage signaling to restrict bacterial growth. J774 murine macrophages were transiently transfected with Myc-SpyA or DsRed-SpyA expression vector followed by infection with SpyA-deficient GAS (see Fig. S3B). Macrophages expressing SpyA (Myc-SpyA and DsRed-SpyA) exhibited reduced bacterial burden compared to control cells (untransfected and DsRed transfected). Reduced bacterial burdens in SpyA-transfected cells and SpyA-expressing *S. aureus* corresponded to higher lactate dehydrogenase (LDH) activity in BMDMs during infections (see Fig. S3C and E). Cells expressing the catalytically dead SpyA$_{E187A}$ mutant showed higher bacterial burdens and lower LDH release similar to those observed with the $\Delta spyA$ mutant (Fig. 1D). We conclude that expression of SpyA, but not of an active-site mutant of the toxin, can increase macrophage bacterial clearance.

SpyA promotes cell death and caspase-3 activation in a manner independent of mitogen-activated protein kinase (MAPK) and NF-κB signaling. Initiation of programmed cell death by host immune cells can limit bacterial infection (reviewed in references 16 and 26). Measuring cell viability using calcein-AM (which stains live cells) and ethidium homodimer-1 (which stains ruptured cells), we saw significantly less death after 4 h in $\Delta spyA$-infected BMDMs than in those infected with the WT or complemented GAS strains (Fig. 2A). LIVE/DEAD cell staining illustrated rounded and shrunken morphologies consistent with
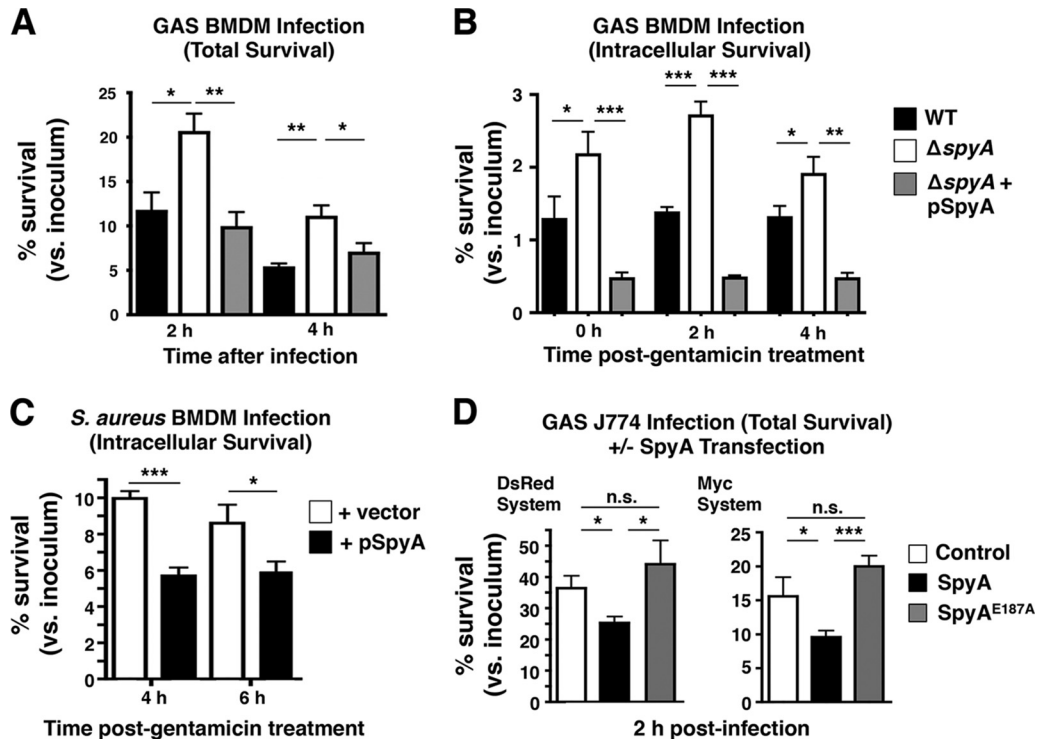
FIG 1 SpyA-deficient GAS bacteria evade macrophage killing. To measure total and intracellular killing, BMDMs isolated from C57BL/6 mice were activated through overnight incubation in DMEM supplemented with 2% FBS. (A) Total killing was measured by recovering total CFU of cells infected with GAS (AP) at an MOI of ~10 after 2 and 4 h. (B) Intracellular killing was assessed by recovering CFU from cells infected with GAS for 30 min followed by 100 μg/ml of gentamicin treatment (1 h); levels of internalized bacteria were monitored over 2 and 4 h in serum-free media. (C) BMDMs were infected with *S. aureus* RN4220 at an MOI of ~5, and intracellular killing was monitored at 4 and 6 h. (D) Transfected J774 cells were infected with ΔspyA GAS for 2 h in 2% FBS media for a total killing assay. Data shown are representative of the results of multiple repeats. Error bar; SEM. *, $P < 0.05$; **, $P < 0.01$; ***, $P < 0.001$; n.s. = not significant; $n = 3$ (Student's two-tailed unpaired t test or one-way ANOVA and Tukey's multiple-comparison test).

the presence of dying or dead cells in macrophages infected with the WT strain or the complemented strain. On the other hand, many cells infected with ΔspyA remained viable, with spreading cell morphology similar to that seen with uninfected cells (Fig. 2A). Dead-cell counts from multiple experiments showed 40% to 50% higher death in BMDMs infected with WT and complemented strains than in those infected with a ΔspyA strain (Fig. 2B). Corroborating these results, lactate dehydrogenase (LDH) release, another marker of cytotoxicity, was significantly reduced during ΔspyA mutant infection (Fig. 2C).

Two major types of programmed cell death have been described: apoptosis and pyroptosis. Each finely orchestrated process can be activated upon recognition of unique microbial virulence structures through Toll-like receptors (TLRs) or NOD-like receptors (NLRs) (reviewed in reference 16). Through these pattern recognition pathways, pathogen exposure stimulates signaling cascades involving mitogen-activated protein kinase (MAPK) and p65 nuclear factor-kappa B (NF-κB) pathways; activated NF-κB subsequently modulates downstream targets to induce apoptotic or pyroptotic cell death (reviewed in reference 16). To ascertain whether SpyA induces cell death via MAPK and NF-κB signaling, we examined the expression level of active forms phospho-p44/42 MAPK (extracellular signal-regulated kinase 1 and 2 [ERK1/2]) (Fig. 2D) and phospho-NF-κB/p65 (Fig. 2E). SpyA did not alter the abundance of either active protein, suggesting that SpyA generates macrophage cytotoxicity in a TLR-independent

manner. To decipher whether SpyA-induced cell death is linked to apoptosis, we examined apoptosis-inducing factor (AIF), cytochrome C, and caspase-3. While GAS infection did not alter AiF expression (Fig. 2F), a significant increase in cytochrome C abundance followed infection with the WT strain but not the ΔspyA strain (Fig. 2G). Caspase-3 was also specifically activated in the presence of SpyA, as demonstrated by the increased cleavage shown in Western blot analysis (Fig. 2H). This result was verified in a commercial assay, which utilizes fluorescent substrate rhodamine 110 [bis-(N-CBZ-L-aspartyl-L-glutamyl-L-valyl-aspartic acid amide)] (Z-DEVD-R110) to measure the activity of caspase-3 and caspase-7 (Fig. 2I).

SpyA stimulates a caspase-1-dependent inflammatory response and IL-1β production in macrophages. As SpyA induced macrophage cell lysis and LDH release, a frequent readout for proinflammatory cell death (23, 27), we asked if SpyA contributed to release of cytokines associated with bacterial clearance. Activation of caspase-1, a key regulator of pyroptosis, was measured using fluorescent probe 6-carboxyfluorescein (FAM) YVAD-fluoromethyl ketone (FMK). The proportion of the FAM YVAD-FMK-stained population was markedly reduced in ΔspyA-infected BMDMs compared to WT-infected BMDMs after 2 h (3% versus 18%) (Fig. 3A and B). Active caspase-1 p10 subunit levels were also diminished in ΔspyA-infected cell lysates and supernatants, which contained mostly noncleaved pro-caspase 1 (Fig. 3C). To characterize GAS association with active caspase-1,
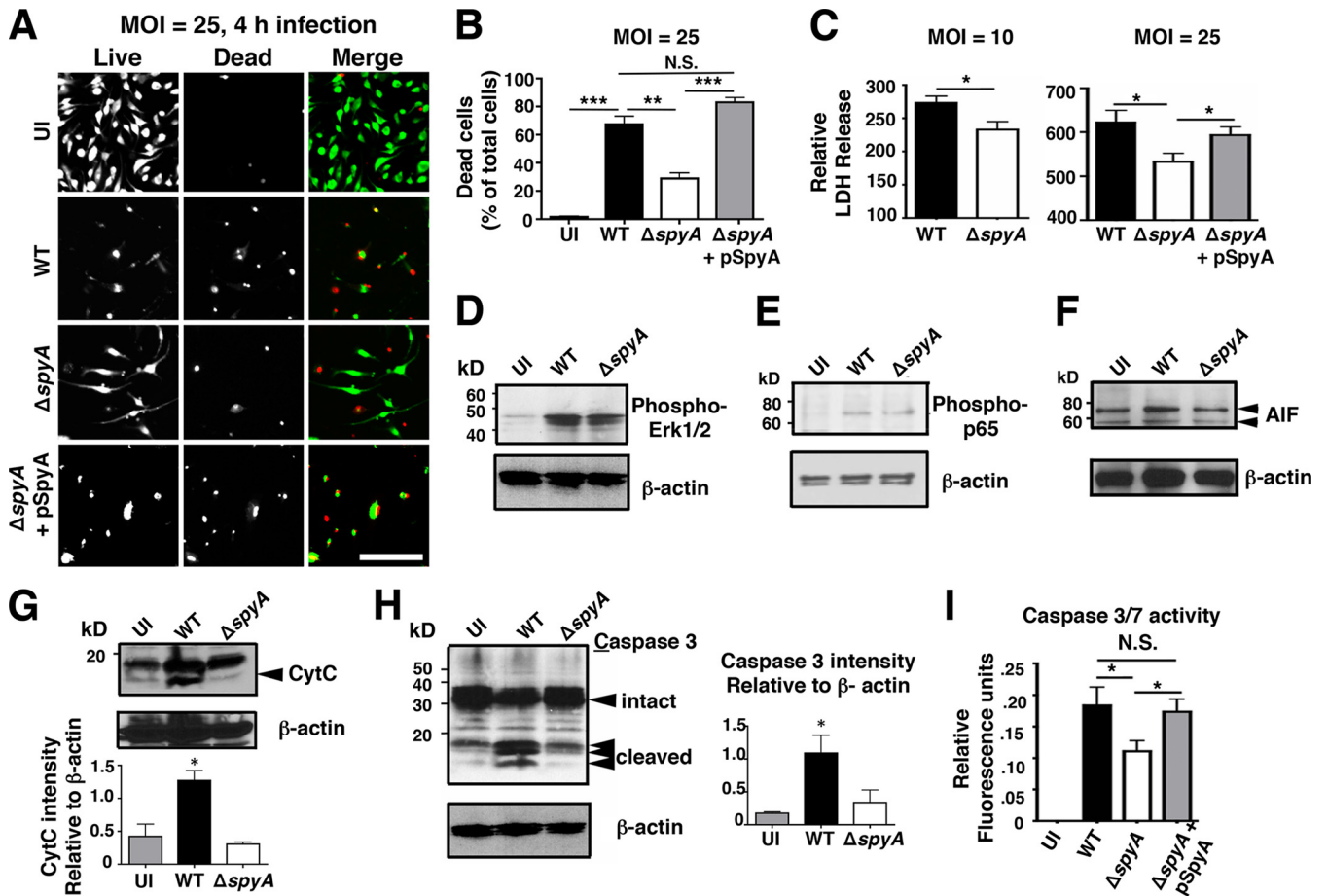
FIG 2 SpyA promotes cell death and caspase-3 activation in a manner independent of MAPK and NF-κB signaling. (A) LIVE/DEAD staining illustrating BMDM viability after 4 h of GAS (AP) infection. Cells were infected at an MOI of ~25 or remained uninfected (UI). Scale bar, 100 μM. (B) Numbers of dead cells were counted from multiple field of views (n = 12). (C) Relative levels of LDH release (percentages compared to uninfected [UI] cells). Δ*spyA*-infected BMDMs exhibit reduced 2-h cell cytotoxicity at an MOI of 10 or 25. Infection with the SpyA-complemented strain restored LDH release to the WT level (n = 4). Error bars, SEM. *, P < 0.05; **, P < 0.01; ***, P < 0.001 (Student's two-tailed unpaired t test). (D to H) Western blot analysis of whole BMDM lysates after 2 h of GAS infection. β-Actin was used as a loading control. (D) Phospho-ERK1/2 (42 or 44 kDa). (E) Phospho-p-p65 (65 kDa). (F) Apoptosis-inducing factor (AIF; 58 or 68 kDa). (G) Cytochrome c (15 kDa). (H) Caspase-3 (FL, full length [35 kDa]; CLVD, cleaved [17 or 19 kDa]). (I) Capsase-3 and caspace-7 (Caspace-3/7) activity assay. Error bars, SEM. *, P < 0.05; n = 4 (Student's two-tailed unpaired t test).

we immunostained bacteria using anti-M1 protein antibody coupled with FAM YVAD-FMK staining. While a large population of WT bacteria colocalized with active caspase-1, reduced colocalization was observed with Δ*spyA* GAS (see Fig. S4 in the supplemental material). Caspase-1 activation is required for secretion of proinflammatory cytokines IL-1β and TNF-α, which is downstream of IL-1β. We found that Δ*spyA* GAS-infected BMDMs produced less transcript (measured by reverse transcription-PCR [RT-PCR]) and protein (measured by enzyme-linked immunosorbent assay [ELISA]) for both IL-1β and TNF-α (Fig. 3D and E). Additionally, BMDMs infected with SpyA-expressing *S. aureus* showed 5-fold-increased IL-1β secretion compared to those infected with control *S. aureus* (Fig. 3F). Together, these results indicate that SpyA contributes to caspase-1-dependent IL-1β release by BMDMs.

GAS SpyA expression is associated with increased bacterial clearance and reduced mortality in mice. Finding that SpyA-mediated proinflammatory IL-1β release is important for bacterial clearance by BMDMs, we investigated whether these results

could be recapitulated in an animal systemic infection model. When CD1 mice were challenged intravenously with GAS (2 × 10^5 to 4 × 10^5 CFU), we found that animals challenged with Δ*spyA* mutants suffered significantly higher mortality than those infected with WT GAS (Fig. 4A). Death in Δ*spyA* mutant-infected mice was observed as early as 2 days postinfection, whereas mortality of the WT-infected mice did not begin until 4 days postinfection. Twenty days postinfection, 60% of the WT strain-infected mice survived whereas only 30% of the Δ*spyA* mutant-infected mice survived (Fig. 4A). To assess severity of disease, we enumerated bacterial CFU from heart, spleen, brain, lung, and blood 2 days postinfection and found that CFU levels in organs from animals infected with the Δ*spyA* mutant were 10-fold to 20-fold higher than the levels in those infected with the WT strain (Fig. 4B and S5). Higher titers of Δ*spyA* GAS were recovered from spleen as early as 12 h postinfection and from blood by 24 h postinfection (see Fig. S5 in the supplemental material). This corroborates our finding of higher CFU levels recovered from Δ*spyA* mutant-infected BMDMs (Fig. 1A and B). Furthermore, mice infected
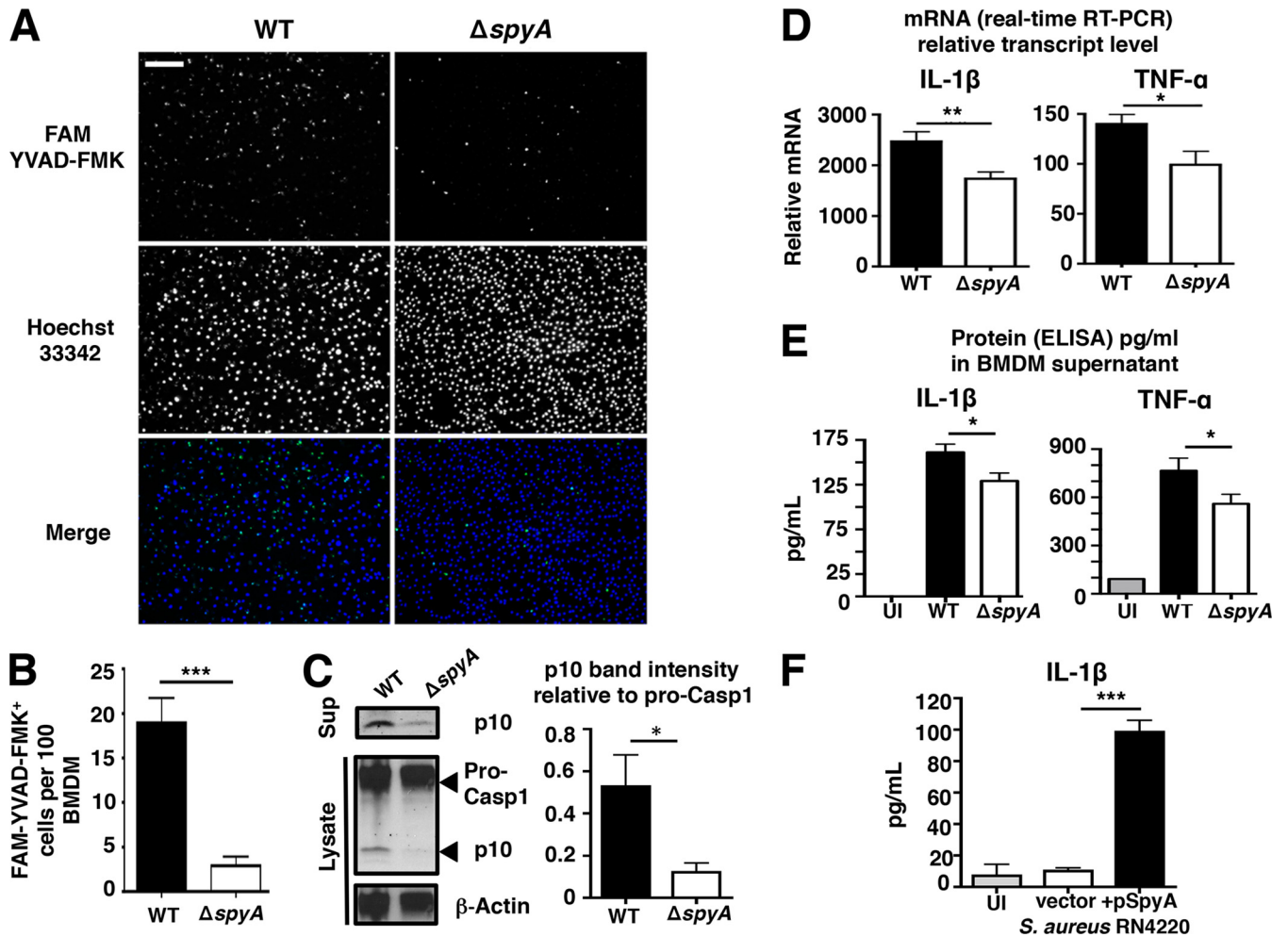
FIG 3 SpyA stimulates a caspase-1-dependent inflammatory response and IL-1β production in macrophages. (A) BMDMs were infected with GAS (AP) at an MOI of ~10. At the end of the assay, cells were washed and stained for 1 h with FAM YVAD-FMK to visualize activated caspase-1 (green) and for 5 min with Hoechst 33342 to visualize DNA (blue) under an epifluorescent microscope. Scale bar, 100 μm. (B) Quantification of FMK YVAD-FMK-positive cells (per 100 cells) from multiple random fields of view (*n* = 10) per sample. (C) Western blot illustrating the abundance of pro-caspase-1 and its p10 subunit in GAS-infected BMDM cell lysates and caspase-1 p10 subunit released in the supernatants (Sup). Data represent densitometry quantifications illustrating average levels of active caspase-1 p10 expression in lysates and supernatants relative to pro-caspase 1 expression. Error bars, SEM. *, *P* < 0.05 (*n* = 3). Experiments were performed in duplicate using BMDMs isolated from four different C57BL/6 mice. (D and E) Real-time qPCR (D) and ELISA (E) quantification of IL-1β and TNF-α transcripts and proteins produced by BMDMs infected with GAS 2 h after total killing (*n* > 3). (F) IL-1β released by BMDMs after 4 h infection with *S. aureus* RN4220 expressing pSpyA or control vector (*n* = 4). Error bars, SEM. *, *P* < 0.05; **, *P* < 0.01; ***, *P* < 0.001 (Student's two-tailed unpaired *t* test). UI, uninfected.

with the pSpyA-complemented mutant strain exhibited reduced bacterial colonization of heart and lung compared to those infected with the Δ*spyA* mutant strain (Fig. 4C). Corresponding to the increase in bacterial burden, Δ*spyA* mutant-infected mice failed to generate a robust inflammatory response during early infection (6 h), as levels of IL-1β and other proinflammatory cytokines, including TNF-α and IL-6, were significantly lower in those mice than in the WT strain-infected mice (Fig. 4D). However, as the infection progressed to 24 and 48 h, the level of proinflammatory cytokines in Δ*spyA* mutant-infected mice became significantly elevated, tracking the bacterial burden, severity, and lethality of systemic disease observed in these animals (Fig. 4D).

GAS SpyA activation of a caspase-1-dependent inflammasome response is required for bacterial clearance by cultured BMDMs and *in vivo*. We next explored whether the SpyA-induced caspase-1-dependent IL-1β proinflammatory signaling

in BMDMs and *in vivo* (Fig. 3E and 4D) correlated with the observed decrease in bacterial recovery (Fig. 1A and B and 4B). BMDMs were treated with general pan-caspase inhibitor ZVAD followed by GAS infection. As a result of interference with multiple caspase activities, recovery of WT GAS was augmented to a level consistent with Δ*spyA* mutant infection (Fig. 5A); similar results were obtained with caspase-1 and caspase-4 Pan-Caspase inhibitor Ac-YVAD-CHO (Fig. 5A). To validate a contribution of caspase-1 in promoting macrophage bacterial killing, we repeated the challenge using BMDMs from casp-1$^{-/-}$ casp-11$^{-/-}$ mice (referred to here as Casp-1$^{-/-}$). Through Western blot analysis and YVAD-FMK staining, we confirmed that these mice express neither pro-caspase-1 nor active caspase-1 in their BMDMs (see Fig. S6A and B in the supplemental material). In WT BMDMs, Δ*spyA* mutant infection was associated with lower LDH release levels and higher bacterial survival levels than those seen with the
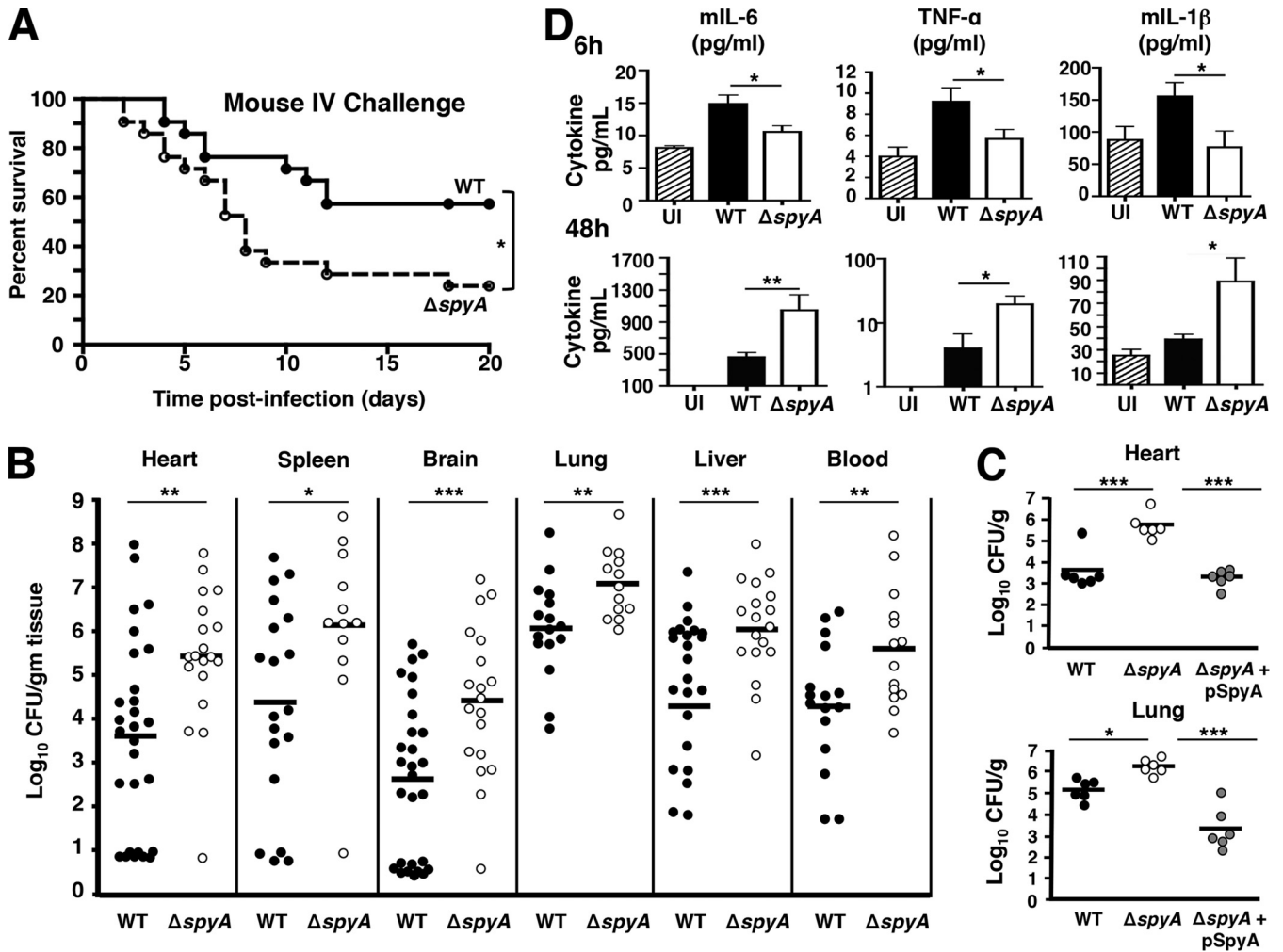
FIG 4 GAS SpyA expression is associated with increased bacterial clearance and reduced mortality in mice. CD1 mice were infected with 2×10^5 to 4×10^5 CFU of WT, $\Delta spyA$, or $\Delta spyA$ plus pSpyA GAS (AP) via tail-vein injection. (A) Survival kinetics of infected mice monitored over 20 days (WT strain $n = 20$, $\Delta spyA$ strain $n = 21$). *, $P = 0.02$. Statistical significance was evaluated using the log rank test with a 95% confidence interval. (B) Bacteria recovered from organs or blood of GAS-infected mice 48 h postinfection for CFU enumeration to assess bacterial burden ($n > 12$). (C) CFU levels recovered from heart and lung of mice infected with $\Delta spyA$ plus pSpyA GAS (48 h) are significantly lower than those from $\Delta spyA$ mutant-infected mice ($n = 6$). (D) ELISA of proinflammatory cytokines from mouse blood serum isolate 6 h and 48 h postinfection ($n = 5$ to 9). UI = uninfected control, WT = wild-type GAS. Error bars, SEM. *, $P < 0.05$; **, $P < 0.01$; ***, $P < 0.001$ (Student's two-tailed unpaired t test).

WT GAS strain. The LDH release result was reversed in BMDMs from Casp-1$^{-/-}$ mice, which showed impaired killing of GAS (Fig. 5B), consistent with the result seen with caspase-1 inhibitor treatment (Fig. 5A). These findings suggest that bacterial killing is significantly improved by caspase-1-mediated proinflammatory cell death.

In addition to caspase-1 processing, IL-1β processing is often associated with inflammasome complexes comprised of NLRP3 and adaptor protein ASC. These components are central caspase-1 regulators that rapidly oligomerize to form the NLRP3 inflammasome and that mediate IL-1β signaling and proinflammatory cell death upon bacterial stimulation (14, 16). Consistent with findings in Casp-1$^{-/-}$ BMDMs, the survival advantage of the $\Delta spyA$ mutant over the WT GAS strain was eliminated in Nlrp3$^{-/-}$, Asc$^{-/-}$, and IL-1β$^{-/-}$ BMDMs (Fig. 5C). With IL-1β production blocked in Casp1/NRLP3/ASC-deficient macrophages (Fig. 5D), the survival advantage of the $\Delta spyA$ mutant over

the WT GAS strain was eliminated, likely due to a lack of IL-1β to trigger recruitment of antimicrobial effectors or of proinflammatory cytokines to restrict bacterial survival (14, 16, 17).

Since SpyA stimulated caspase-1-derived IL-1β release to attenuate GAS growth in assays of macrophages, we predicted that blockade of IL-1β signaling *in vivo* would result in greater bacterial growth and accelerated mortality. Anakinra (Kineret; 100 mg/kg of body weight), a nonglycosylated recombinant human IL-1β receptor antagonist, was administered at 12-h intervals to block IL-1β signaling in mice (28). Mice treated with anakinra succumbed significantly earlier to WT GAS infection and suffered higher bacterial loads than phosphate-buffered saline (PBS)-treated control mice (Fig. 5E). No significant differences in the mortality levels of $\Delta spyA$ mutant- and WT GAS-infected mice were observed in the setting of anakinra treatment (Fig. 5E), with similar bacterial loads enumerated in heart, spleen, lung, and liver of anakinra-treated mice, regardless of the presence or absence of
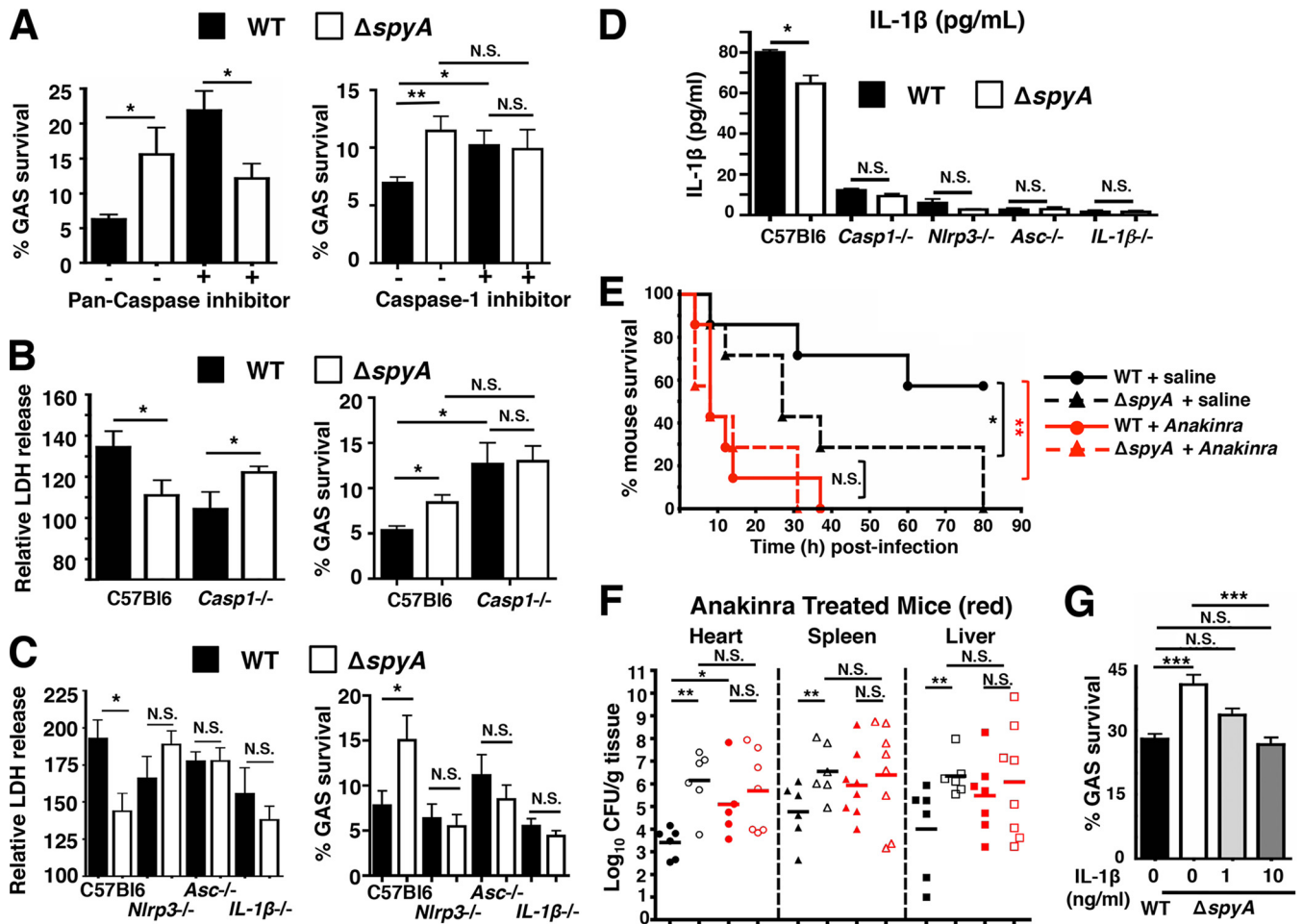
FIG 5 GAS SpyA activation of a caspase-1-dependent inflammasome response is required for bacterial clearance by cultured BMDMs and *in vivo*. (A) BMDMs were coincubated with GAS (AP) at an MOI of 20 plus 10 μM pan-caspase inhibitor zVAD-FMK (ZVAD) or 25 μM caspase-1 inhibitor Ac-YVAD-CHO (YVAD) for 2 h. Data shown are representative of the results of multiple experiments. (B) Relative levels of LDH release (percentages compared to levels in uninfected [UI] cells; left panel) and bacterial killing (right panel) by WT and Casp-1⁻/⁻ BMDMs 2 h postinfection. (C) Relative levels of LDH release (left panel) and bacterial killing (right panel) 2 h postinfection (MOI = 5) by BMDMs isolated from wild-type (C57bl6), Nlrp3⁻/⁻, Asc⁻/⁻, and IL-1β⁻/⁻ mice (n = 3). Data shown are representative of the results of two or more animals. (D) ELISA shows IL-1β secreted by BMDMs isolated from wild-type (C57bl6), Nlrp3⁻/⁻, Asc⁻/⁻, and IL-1β⁻/⁻ mice after 2 h coincubation with GAS at an MOI of 20. Data shown are representative of the results of two animals. (E) CD1 mice were infected with 7 × 10⁵ CFU of WT or ΔspyA GAS (AP) via tail-vein injection (n = 7 per group). Immediately after infection, anakinra (IL-1 receptor antagonist) was subcutaneously injected at 100 mg/kg over a 12-h interval until the end of survival curve. WT plus saline solution versus ΔspyA plus saline solution, *, P = 0.04; WT plus saline solution versus WT plus anakinra. **, P = 0.0036; WT plus anakinra versus ΔspyA plus anakinra, P = 0.06; ΔspyA plus saline solution versus ΔspyA plus anakinra, P = 0.07 (log rank test with 95% confidence interval); N.S., not significant (P > 0.05). (F) GAS-infected mice (n = 8 to 10) were sacrificed 2 days postinfection; heart, spleen, and liver were harvested for CFU enumeration; no statistically significant differences were observed between WT and ΔspyA-infected animals that received anakinra treatment or for ΔspyA-infected animals with saline solution treatment. Closed symbols = WT; open symbols = ΔspyA. Black = control mice, red = anakinra-treated mice. Error bars, SEM. Statistical analysis: *, P < 0.05; N.S., not significant (P > 0.05) (Student's two-tailed unpaired t test). (G) BMDMs in RPMI plus 2% FBS were treated with 1 or 10 ng/ml of recombinant mouse IL-1β (PeproTech, Rocky Hill, NJ) at the time of infection. Cells were washed and CFU recovered 2 h postinfection to assess bacterial killing. Error bars, SEM. *, P < 0.05; **, P = 0.01; ***, P < 0.001; NS, not significant; n = 3 (Student's unpaired two-tailed t test).

SpyA expression (Fig. 5F). When recombinant IL-1β (10 ng/ml) was provided to BMDMs during macrophage killing assays performed with the ΔspyA mutant, bacterial killing was restored to the levels seen with WT GAS infection (Fig. 5G). Collectively, these results indicate that SpyA stimulates IL-1β production as a critical host defense response to impede bacterial growth in macrophages and *in vivo*.

***Pseudomonas aeruginosa* ADP-ribosyltransferase toxin A also triggers an inflammasome-dependent macrophage response to enhance bacterial killing.** *P. aeruginosa* exotoxin A (PEA) is a well-characterized C3 family ADP-ribosyltransferase

that targets host elongation factor 2 to induce a block in translation elongation (29) and programmed cell death (30, 31). Given the functional similarity to SpyA, we investigated whether the bacterial clearance triggered by SpyA-mediated proinflammatory cell death could be recapitulated by PEA. We found PEA to induce macrophage cell death as measured by LDH release while upregulating transcription and protein expression of IL-1β and TNF-α by BMDMs (Fig. 6A to E). BMDMs infected with a PEA-deficient (ΔtoxA) mutant released significantly less LDH 2 h postinfection than WT *P. aeruginosa*-infected cells (Fig. 6F), and the ΔtoxA mutant had greater total and intracellular survival (Fig. 6G and H)
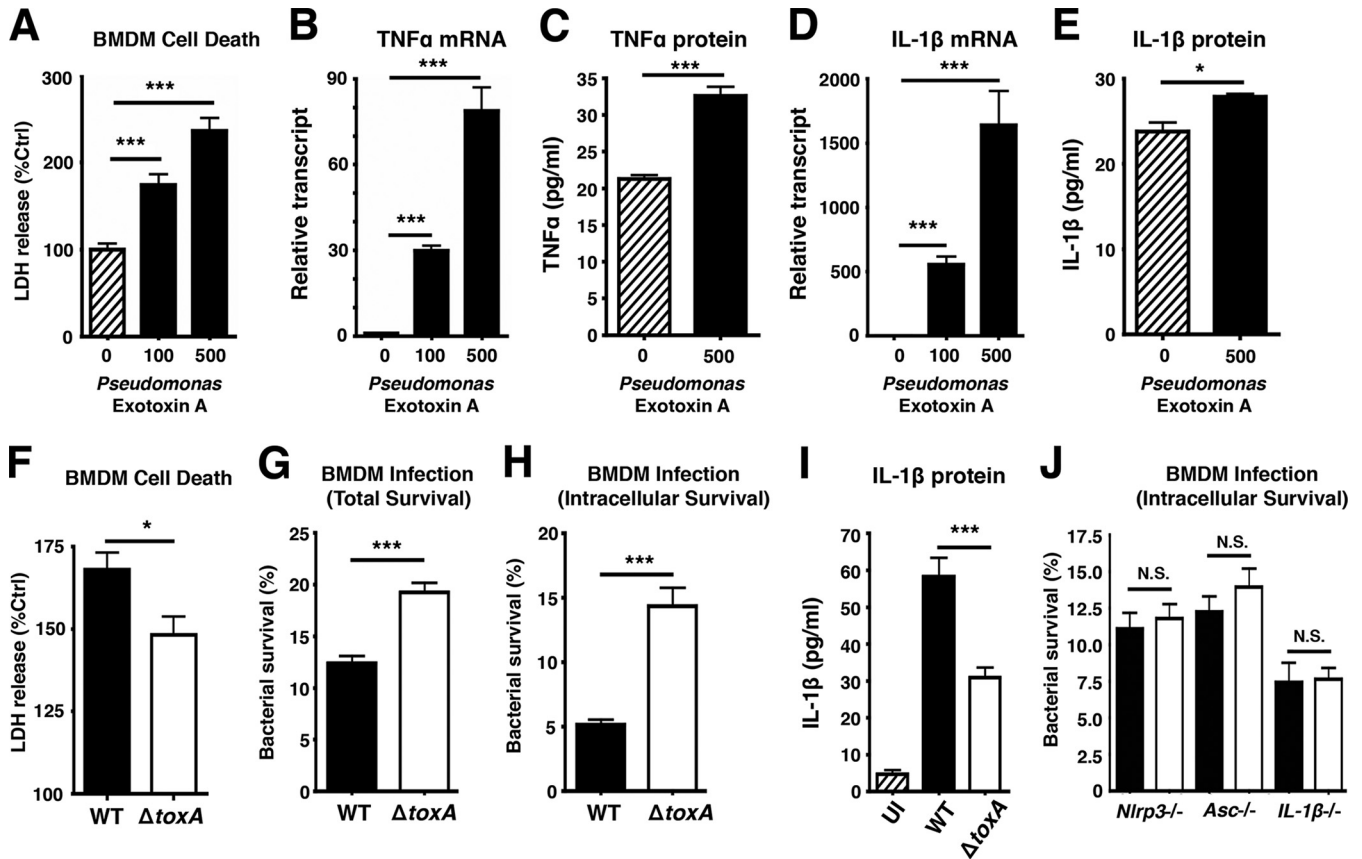
FIG 6 *Pseudomonas aeruginosa* ADP-ribosyltransferase exotoxin A triggers an inflammasome-dependent macrophage response to enhance bacterial killing. BMDMs were seeded in 24 wells in 2% FBS media a day before infection. (A) LDH released by BMDMs treated with 100 ng or 500 ng of *P. aeruginosa* exotoxin A (PEA) for 18 h. (B to E) RNA and supernatants from BMDMs were isolated for real-time qPCR and ELISA to assess transcript and protein levels of TNF-α and IL-1β in BMDMs treated with PEA. (F) LDH assay of supernatants harvested from BMDMs 2 h after *P. aeruginosa* infection ($n = 4$). (G and H) Total and intracellular killing of *P. aeruginosa* infected for 30 min at an MOI of ~20, followed by a 1-h streptomycin treatment (150 μg/ml). Cells were washed and incubated in serum-free media for 2 h to establish intracellular killing. (I) ELISA of IL-1β produced by *P. aeruginosa*-infected BMDMs 2 h postinfection. (J) BMDMs from Nlrp3$^{-/-}$, Asc$^{-/-}$, and IL-1β$^{-/-}$ mice were isolated to assess intracellular killing of *P. aeruginosa* (2 h post-gentamicin treatment). Error bars, SEM. *, $P < 0.05$; **, $P < 0.01$; ***, $P < 0.001$; $n = 3$ (Student's unpaired *t* test or one-way ANOVA followed by Dunnett's test).

and reduced IL-1β induction (Fig. 6I). Differences in bacterial recovery between WT *P. aeruginosa* infection and Δ*toxA* mutant infection were abolished in BMDMs from NLRP3, ASC, and IL-1β knockout mice (Fig. 6J). These results suggest that bacterial ADP-ribosyltransferase toxins could be a common pathogen-associated phenotype recognized by the innate immune system through inflammasome complexes in macrophages to initiate proinflammatory cell death, ultimately augmenting host bacterial clearance.

DISCUSSION

IL-1β-dependent proinflammatory signaling is recognized as a key innate immune process supporting host defense against microbial infections. The importance of IL-1β in restricting microbial replication in macrophages and *in vivo* has been highlighted in a diverse range of intracellular pathogens, including *Legionella*, *Salmonella*, *Mycobacterium*, *Yersinia*, and *Shigella* spp., and even *Leishmania* parasites, to name a few (14, 16, 18, 23, 27, 32). These intracellular microbes trigger caspase-1-dependent inflammasome activation, which leads to IL-1β secretion and initiates lytic cell death. Production of IL-1β is also essential to control intracellular growth of these microbes (14, 16, 18, 32). GAS bac-

teria reportedly exhibit the capacity to stimulate the NLRP3 inflammasome via SLO, a pore-forming cytotoxin (24), with unknown implications for invasive disease pathogenesis. Here we provide evidence that GAS SpyA, a C3 ADP-ribosyltransferase, activates a caspase-1-dependent IL-1β inflammatory response. SpyA mediates caspase-1 signaling to stimulate the IL-1β cytokine release necessary for a subsequent increase in bacterial killing of invasive M1T1 GAS in macrophages. Macrophages undergoing immunological cell death may release fewer bacteria, which could result in our observed phenotype of less bacterial recovery in GAS-infected macrophages (23).

SpyA contributes to bacterial clearance through canonical caspase-1-dependent processing to promote IL-1β activation and by increasing IL-1β transcription. Concurrent with increased recovery of the Δ*spyA* mutant during infection, Δ*spyA* mutant-infected macrophages displayed markedly reduced caspase-1 activity relative to WT-infected cells. In addition to caspase-1, SpyA appears to activate caspase-3 in a cytochrome C-dependent manner. Caspase-3 is traditionally associated with apoptosis and has also been characterized as a component of a strategy to limit replication of certain intracellular bacteria (33, 34). For the pathogen

GAS, accelerated phagocyte apoptosis triggered by streptolysin is a known GAS virulence mechanism (35). Because apoptosis is immunologically silent (13, 16, 20), we suspect that its activation by SpyA is secondary to the propyroptotic effect in the contexts considered in this study.

Along with showing a diminished ability to kill GAS, $\Delta spyA$ mutant-infected macrophages released less LDH, TNF-α, and IL-1β, consistent with impaired immune defense, thereby limiting the host's ability to restrict bacterial growth. The effect of SpyA in stimulating an innate host response that restricts bacterial survival is evident, as animals infected with SpyA-deficient GAS exhibited greater bacterial burden and mortality than those infected with the WT pathogen. In contrast, expression of SpyA in *S. aureus* or transgenic expression in macrophages significantly enhanced bacterial clearance. Our findings in GAS SpyA are consistent with the results seen with *Legionella* flagellin, which also activates caspase-1-dependent cytotoxicity in macrophages to restrict intracellular bacterial growth (23). The same study also showed that expression of *Salmonella* flagellin in flagellin-deficient *Legionella* isolates restored caspase-1-dependent cytotoxicity to WT levels.

To delineate the importance of IL-1β in restricting bacterial growth, we examined caspase-1-, NLRP3-, and ASC-deficient BMDMs and found that SpyA-induced bacterial killing and proinflammatory cell death were diminished in the cells that lacked the ability to secrete active IL-1β. Similar observations were made for *Leishmania* and *Mycobacterium* spp. in studies in which macrophages and mice deficient in IL-1R and caspase-1 were impaired in defense against infections (18, 32). The critical role of IL-1β in clearance of systemic GAS infection was highlighted upon pharmacological treatment of infected mice with the IL-1β antagonist anakinra. The overall bacterial burden in multiple organs of WT GAS-infected mice was higher upon anakinra treatment, a difference especially pronounced in the heart tissue (Fig. 5F). In contrast, addition of purified IL-1β to $\Delta spyA$ mutant-infected BMDM restored bacterial killing to WT levels. Therefore, our study results suggest that generation of IL-1β through caspase-1 activation is important for limiting bacterial replication and that blockade of IL-1β signaling increases bacterial burden in multiple organs to accelerate mortality.

It remains unclear precisely how SpyA is recognized by the inflammasome family to promote caspase-1-dependent IL-1β activation. Based on our finding that cells transfected with an active-site mutant allele, SpyA$_{E187A}$, did not mediate effective bacterial clearance, we suspect that SpyA triggers IL-1β release related to perturbations caused by its ADP-ribosyltransferase activity on multiple host cell targets (12). This possibility is supported by our finding that *P. aeruginosa* exotoxin A (PEA), a C3-like ADP ribosyltransferase toxin like SpyA, also rapidly stimulates LDH and IL-1β release by macrophages. Moreover, this toxin-mediated proinflammatory cytotoxicity improves bacterial clearing by BMDMs. We have initiated collaborative biochemical studies to identify the specific host substrate(s) that interacts directly with SpyA to activate caspase-1-dependent cytotoxicity.

Our use of the AP (*covS* mutant) GAS strain focused our attention on the bloodstream stage of the infection, and our data should not be extrapolated to suggest that SpyA stimulates GAS clearance at other distinct stages or foci of infection. Researchers who performed earlier studies speculated that in early, localized infections, SpyA effects that cause epithelial cell damage such as cytoskeletal protein rearrangement and programmed cell death

(9, 10, 12) may promote survival within a skin abscess. Furthermore, during the initial stages of colonization and mucosal infection (e.g., pharyngitis), it is possible that GAS activation of host inflammatory responses results in preferential clearance of normal microflora, upon which the pathogen with its larger arsenal of immune resistance factors can occupy the evacuated niche, similar to a recent paradigm shift in our understanding of *Salmonella* gastrointestinal infection (36, 37).

It is perhaps counterintuitive that GAS would produce a toxin that seemingly attenuates virulence in BMDMs and in the *in vivo* models used in this particular study. *Legionella* flagellin and Ipaf (a homolog of NAIP5) and *Yersinia* YopJ (an acetyl-transferase) also trigger caspase-1 expression, resulting in higher levels of LDH release and restriction of bacterial growth in macrophages, consistent with our findings with GAS SpyA (23, 27). The role of a toxin of a potentially pathogenic bacterium in promoting virulence versus immune activation is likely to vary, based on the site, stage, and magnitude of infection, from simple colonization to systemic disease. An important emerging area of innate immune research is how the immune system recognizes toxic activities to elicit protective host defense programs. For example, the pore-forming alpha-toxin of *S. aureus* elicits a NOD2-dependent, IL-1β-amplified, and IL-6-mediated protective immune response (38), anthrax lethal factor-mediated cell death triggered a protective ATP- and IL-1β-mediated host defense program (39), and pneumococcal neuraminidase is detected with ERK phosphorylation, NF-κB activation, interleukin-8 release, and neutrophil extracellular trap formation leading to pathogen clearance in a lung infection model (40). Only by understanding such dualities can we explain how the vast majority of encounters with pathogens are successfully resolved by innate host defenses.

MATERIALS AND METHODS

Animals. Female CD1 mice aged 6 to 8 weeks (Charles River Laboratory, Hollister, CA) were infected with 3×10^5 to 5×10^5 CFU of GAS bacteria (AP strains) in PBS via tail-vein injection. For survival assays, mice ($n = 21$) were monitored over a period of 20 days for mortality. For measurement of bacterial burden in organs, mice were euthanized 2 days postinfection by CO_2 asphyxiation; organs (liver, spleen, brain, lung, heart, and blood) were homogenized (using a Roche homogenizer) in 1 ml phosphate-buffered saline (PBS) with 1-mm-diameter zirconia/silica beads (BioSpec Products), serially diluted in PBS, and plated on Todd-Hewitt agar (THA) for CFU enumeration. All animal experiments were conducted under approved protocols and according to the regulations and guidelines of the Institutional Animal Care and Use Committee at the University of California, San Diego.

Bacterial strains and culture conditions. Human GAS serotype M1T1 5448 was isolated from a patient with necrotizing fasciitis and toxic shock syndrome (25). An isogenic in-frame allelic exchange $\Delta spyA$ knockout mutant was constructed by an established protocol (41). Animal-passaged strains were generated as previously described (42). Plasmid-based complementation of the $\Delta spyA$ (AP) strain with pDCerm-SpyA (designated $\Delta spyA$ plus pSpyA) was achieved using prior protocols (43). For experiments, GAS were grown at 37°C overnight in Todd-Hewitt broth (THB) in stationary culture with 5 μg/ml erythromycin for complemented strains containing the pDC$_{erm}$ plasmid. All infections were performed using the GAS AP strains unless stated otherwise. Heterologous expression of SpyA in *S. aureus* RN4220 was achieved by transforming *S. aureus* RN4220 with pDC$_{erm}$ or pDC$_{erm}$-SpyA vectors following a previous protocol (44). Transformed colonies were selected using 3 μg/ml of erythromycin and confirmed by PCR and RT-PCR analyses. The *P. aeruginosa* PA14 WT and $\Delta toxA$ strains were grown in Luria Bertani

(LB) broth at 37°C shaking at 220 rpm overnight. The Δ*toxA* mutant was grown in LB plus 15 µg/ml gentamicin.

Macrophage cultures. BMDMs were isolated from the femurs and tibia of 8-to-12-week-old WT C57BL/6 mice (Jackson Laboratory) and *casp-1/11*$^{-/-}$ (provided by R. Flavell), Asc$^{-/-}$, or Nlrp3$^{-/-}$ (provided by J. Bertin of Millennium Pharmaceuticals) and IL-1β$^{-/-}$ (provided by D. Chaplin) C57BL/6 mice. Femurs and tibia were flushed with room-temperature Dulbecco's modified Eagle's medium (DMEM), and precursor cells were cultured in DMEM–20% fetal bovine serum (FBS), 20% L929 cell-conditioned media, 1% nonessential amino acids, 1% sodium pyruvate, and 1% penicillin-streptomycin and grown at 37°C in 5% CO$_2$ for 7 days, with changes of media on day 4. Murine J774 macrophages and human THP-1 monocytes were cultured in 10% FBS–RPMI medium. A day prior to infection, cells were seeded in 24-well plates in RPMI medium with 2% FBS and 60 ng/ml phorbol myristate acetate (PMA) (Fisher).

Inhibitor analysis. Prior to infection with GAS, BMDMs were treated with 10 µM pan-caspase inhibitor ZVAD-FMK (Promega) or 25 µM caspase-1-specific inhibitor Ac-YVAD-CHO (Promega). For intracellular killing, inhibitors were introduced after infection and clearance of noninternalized bacteria.

Real-time quantitative PCR. Total bacterial RNA was isolated from pelleted overnight cultures of GAS incubated for 30 min at 37°C using 500 µl of cell lysis buffer (25% glucose, 10 mM EDTA, 100 mM Tris [pH 7.0], 4 mg/ml lysozyme, 40 µg/ml mutanolysin) and resuspended in 1 ml of Trizol (Invitrogen). RNA isolation from mammalian cells was performed according to the standard Trizol protocol as previously described (45). RNA was resuspended in RNase/DNase-free water with TURBO DNase (Invitrogen); 100 ng of RNA was reverse transcribed using an iScript cDNA synthesis kit (BioRad). cDNA (~1 ng) was used for real-time qPCR with iQ SYBR green Supermix or KAPA SYBR qPCR 2× master mix (KAPA Biosystem; catalog no. KM4101) and primers at a final concentration of 200 nM. The primers used in this study were as follows: for murine IL-6 (mIL-6) (F), 5′-TAGTCCTTCCTACCCCAATTTCC-3′; for mIL6 (R), 5′-TTGGTCCTTAGCCACTCCTTC-3′; for mIL-1β (F), 5′-GAAATGCCACCTTTTGACAGT-3′; for mIL-1β (R), 5′-CTGGATG CTCTCATCAGGACA-3′; for mTNF-α (F), 5′-CCCTCACACTCAGAT GATCTTCT-3′; for mTNF-α (R), 5′-CCCTCACACTCAGATGATCTTC T-3′; for β-tubulin (F), 5′-CCCCACTGAGACTGATACATACG-3′; for β-tubulin (R), 5′-CGATCCCAGTAGACGGTCTTG-3′ (control); for spyA (F), 5′-GCGTGATATCGGTGTTTCAC-3′; for spyA (R), 5′-AAAC TGTGCTTGGTGTAGCG-3′; for gyrA (F), 5′-CGACTTGCTTGAACGC CAAA-3′; and for gyrA (R), 5′-TTATCACGTTCCAAACCAGTCAA-3′ (control). Relative transcript levels were calculated after normalization to β-tubulin (for mammalian cells) and gyrase A (for bacteria) using the threshold cycle ($2^{-\Delta\Delta CT}$) method (46).

Cytokine quantification by ELISA. Concentrations of mouse cytokines were measured in culture supernatants from infected BMDMs (2 or 4 h) or in sera of mice infected for 2 days. mIL-6, monocyte chemoattractant protein 1 (MCP-1), mTNF-α, and mIL-1β were detected using ELISA kits (R & D Systems). Assays were performed as triplicates or quadruplicates.

Transient transfection with SpyA expression construct. Murine J774 macrophages were cultured in RPMI medium–10% FBS at 37°C. On the day of transfection, cells were seeded in 24-well plates in DMEM–2% FBS at ~90% confluence. Cells were treated with 2 µg of purified plasmid pCMV-Myc-SpyA, pCMV-Myc-SpyA$_{E187A}$, pEF1α-internal ribosome entry site (IRES)-DsRed-Express2 (DsRed), pEF1α-IRES-DsRed-Express2-SpyA (DsRed-SpyA) or pEF1α-IRES-DsRed-Express2-SpyA$_{E187A}$ (DsRed-SpyA$_{E187A}$) (12) and with JetPEI reagent for macrophage transfection (PolyPlus) according to the manufacturer's protocol. After 24 h of transfection, cells were infected with GAS for macrophage killing assays. The SpyA transcript level in each cell was quantified by real-time qPCR.

Cytotoxicity and LIVE/DEAD assays. The LDH cytotoxicity assay (Promega) was used following the manufacturer's protocol. Supernatants from uninfected or infected macrophages were harvested and diluted 2× or 4× in 96-well plates before being mixed with LDH reagent. LDH release was normalized to the percentage of uninfected cells or cells with transfecting reagent only. Cell viability staining was visualized using a LIVE/DEAD kit for mammalian cells (Invitrogen) following the manufacturer's protocol. The Apo-ONE Homogeneous caspase-3/7 assay (Promega) was performed per the manufacturer's protocol (47).

Macrophage killing assays. Macrophage killing assays were performed as previously described (48), with minor modifications. Briefly, BMDMs were seeded at approximately 5×10^5 cells in 350 µl of DMEM–2% FBS in a 24-well plate. Overnight bacterial cultures were diluted 1:10 and subcultured for 2 to 3 h with shaking. BMDMs were infected with bacteria (GAS, *S. aureus*, or *P. aeruginosa*) at an MOI of 5 to 10. Plates were centrifuged at $600 \times g$ for 5 min to facilitate bacterial contact with macrophages. To assess total macrophage killing, cells were incubated at 37°C for 2 h, washed three times with PBS, detached with 100 µl of 0.05% trypsin, and lysed with 900 µl of 0.025% Triton X-100–PBS. To assess intracellular survival, cells were incubated at 37°C for 30 min, quickly washed once with PBS, and replaced in serum-free DMEM–100 µg/ml gentamicin to kill extracellular bacteria. After 1 h of incubation, cells were rinsed once with PBS and fresh serum-free DMEM for an additional 2 h before treatment with trypsin and Triton X–PBS as described above. Samples were serially diluted in PBS and plated on THB overnight for CFU enumeration. A similar procedure was utilized for THP-1 human monocytes and murine macrophage cell line J774.

Detection of caspase-1 activity. The level of active caspase-1 was detected using a FAM YVAD-fluoromethyl ketone (FMK) staining kit (Immunochemistry Technologies). BMDMs infected with the GAS WT strain or Δ*spyA* mutant were washed and incubated with FAM YVAD-FMK for 1 h at 37°C and for 10 min with Hoescht stain according to the manufacturer's protocol. Active caspase-1 was visualized by the use of an Olympus BX51 fluorescence microscope fitted with appropriate filters, and numbers were counted in multiple fields ($n = 10$) per sample. Experiments were performed in duplicate and repeated at least three times.

Membrane protein isolation and Western blotting. In a 24-well plate, 1×10^6 to 2×10^6 BMDMs were seeded per well in 350 µl of DMEM supplemented with 2% FBS. In a 6-well plate, 2×10^6 BMDMs were seeded per well in 1.5 ml of DMEM supplemented with 2% FBS. Cells were infected with GAS at an MOI of ~10 to ~20, and supernatants were collected for ELISAs. To harvest whole-cell lysates, cells were washed 3 times with PBS and treated with radioimmunoprecipitation assay (RIPA) lysis buffer (45). To isolate membrane fractions, whole-cell lysates were sheared through needles of ascending gauges (18, 22, 25, 26, and 30 gauge). Ruptured cell fractions were centrifuged at $3,500 \times g$ for 5 min. The supernatant was collected and centrifuged at 25,000 rpm at 4°C. The pellet containing the membrane fraction was collected for Western blot analysis using rabbit anti-SpyA (diluted 1:500 in Tris-buffered saline–Tween 20 [TBST]). Protein abundances were determined in whole-cell lysates in RIPA lysis buffer and supernatants collected by trichloroacetic acid (TCA) extraction using the following antibodies: anti-phopho-p65, rabbit anti-phospho-pERK1/2, and rabbit anti-caspase-3 (Cell Signaling Technologies) (diluted 1:1,000 in 5% bovine serum albumin [BSA]–T-BST); mouse cytochrome C (BD Biosciences) (1:500 in TBS); mouse anti-β-actin (Sigma Aldrich) (1:2,000 in TBST); and rabbit anti-caspase-1 p10 (Santa Cruz Technologies) (1:200 in TBST). Enhanced chemiluminescence reagent (PerkinElmer) was used for detection.

Statistical analysis. Experiments were all performed in triplicate and repeated at least twice. Error data represent standard errors of the means (SEM) ($n > 3$) of the results from experimental duplicates, triplicates, or quadruplets. Statistical analysis was performed using Student's unpaired two-tailed t test except for the survival assay, in which statistical significance was evaluated using the log rank test with a 95% confidence interval. Comparisons among three or more samples were evaluated using one-way analysis of variance (ANOVA) followed by the nonparametric Tukey's posttest. Comparisons of multiple samples were evaluated using

ANOVA followed by Dunnett's or Tukey's test (Graph Pad Prism, version 5.03). * ($P < 0.05$), ** ($P < 0.01$), and *** ($P < 0.001$) represent statistical significance.

REFERENCES

1. Carapetis JR, Steer AC, Mulholland EK, Weber M. 2005. The global burden of group A streptococcal diseases. Lancet Infect Dis 5:685–694. http://dx.doi.org/10.1016/S1473-3099(05)70267-X.
2. Aziz RK, Kotb M. 2008. Rise and persistence of global M1T1 clone of Streptococcus pyogenes. Emerg Infect Dis 14:1511–1517. http://dx.doi.org/10.3201/eid1410.071660.
3. Sumby P, Whitney AR, Graviss EA, DeLeo FR, Musser JM. 2006. Genome-wide analysis of group A streptococci reveals a mutation that modulates global phenotype and disease specificity. PLoS Pathog 2:e5. http://dx.doi.org/10.1371/journal.ppat.0020005.
4. Cole JN, Barnett TC, Nizet V, Walker MJ. 2011. Molecular insight into invasive group A streptococcal disease. Nat Rev Microbiol 9:724–736. http://dx.doi.org/10.1038/nrmicro2648.
5. Walker MJ, Hollands A, Sanderson-Smith ML, Cole JN, Kirk JK, Henningham A, McArthur JD, Dinkla K, Aziz RK, Kansal RG, Simpson AJ, Buchanan JT, Chhatwal GS, Kotb M, Nizet V. 2007. DNase Sda1 provides selection pressure for a switch to invasive group A streptococcal infection. Nat Med 13:981–985. http://dx.doi.org/10.1038/nm1612.
6. Cole JN, Pence MA, von Kockritz-Blickwede M, Hollands A, Gallo RL, Walker MJ, Nizet V. 2010. M protein and hyaluronic acid capsule are essential for in vivo selection of covRS mutations characteristic of invasive serotype M1T1 group A streptococcus. mBio 1:e00191-10. http://dx.doi.org/10.1128/mBio.00191-10.
7. Maamary PG, Sanderson-Smith ML, Aziz RK, Hollands A, Cole JN, McKay FC, McArthur JD, Kirk JK, Cork AJ, Keefe RJ, Kansal RG, Sun H, Taylor WL, Chhatwal GS, Ginsburg D, Nizet V, Kotb M, Walker MJ. 2010. Parameters governing invasive disease propensity of non-M1 serotype group A streptococci. J Innate Immun 2:596–606. http://dx.doi.org/10.1159/000317640.
8. Coye LH, Collins CM. 2004. Identification of SpyA, a novel ADP-ribosyltransferase of Streptococcus pyogenes. Mol Microbiol 54:89–98. http://dx.doi.org/10.1111/j.1365-2958.2004.04262.x.
9. Korotkova N, Hoff JS, Becker DM, Quinn JK, Icenogle LM, Moseley SL. 2012. SpyA is a membrane-bound ADP-ribosyltransferase of Streptococcus pyogenes which modifies a streptococcal peptide, SpyB. Mol Microbiol 83:936–952. http://dx.doi.org/10.1111/j.1365-2958.2012.07979.x.
10. Hoff JS, DeWald M, Moseley SL, Collins CM, Voyich JM. 2011. SpyA, a C3-like ADP-ribosyltransferase, contributes to virulence in a mouse subcutaneous model of Streptococcus pyogenes infection. Infect Immun 79:2404–2411. http://dx.doi.org/10.1128/IAI.01191-10.
11. Deng Q, Barbieri JT. 2008. Molecular mechanisms of the cytotoxicity of ADP-ribosylating toxins. Annu Rev Microbiol 62:271–288. http://dx.doi.org/10.1146/annurev.micro.62.081307.162848.
12. Icenogle LM, Hengel SM, Coye LH, Streifel A, Collins CM, Goodlett DR, Moseley SL. 2012. Molecular and biological characterization of streptococcal SpyA-mediated ADP-ribosylation of intermediate filament protein vimentin. J Biol Chem 287:21481–21491. http://dx.doi.org/10.1074/jbc.M112.370791.
13. Franchi L, Muñoz-Planillo R, Núñez G. 2012. Sensing and reacting to microbes through the inflammasomes. Nat Immunol 13:325–332. http://dx.doi.org/10.1038/ni.2231.
14. Hagar JA, Miao EA. 2014. Detection of cytosolic bacteria by inflammatory caspases. Curr Opin Microbiol 17:61–66. http://dx.doi.org/10.1016/j.mib.2013.11.008.
15. Von Moltke J, Ayres JS, Kofoed EM, Chavarría-Smith J, Vance RE. 2013. Recognition of bacteria by inflammasomes. Annu Rev Immunol 31:73–106. http://dx.doi.org/10.1146/annurev-immunol-032712-095944.
16. Bergsbaken T, Fink SL, Cookson BT. 2009. Pyroptosis: host cell death and inflammation. Nat Rev Microbiol 7:99–109. http://dx.doi.org/10.1038/nrmicro2070.
17. Ng TM, Kortmann J, Monack DM. 2013. Policing the cytosol—bacterial-sensing inflammasome receptors and pathways. Curr Opin Immunol 25:34–39. http://dx.doi.org/10.1016/j.coi.2012.11.009.
18. Jayaraman P, Sada-Ovalle I, Nishimura T, Anderson AC, Kuchroo VK, Remold HG, Behar SM. 2013. IL-1beta promotes antimicrobial immunity in macrophages by regulating TNFR signaling and caspase-3 activation. J Immunol 190:4196–4204. http://dx.doi.org/10.4049/jimmunol.1202688.
19. Netea MG, Simon A, van de Veerdonk F, Kullberg BJ, Van der Meer JW, Joosten LA. 2010. IL-1beta processing in host defense: beyond the inflammasomes. PLoS Pathog 6:e1000661. http://dx.doi.org/10.1371/journal.ppat.1000661.
20. Dinarello CA. 1996. Biologic basis for interleukin-1 in disease. Blood 87:2095–2147.
21. Martinon F, Tschopp J. 2007. Inflammatory caspases and inflammasomes: master switches of inflammation. Cell Death Differ 14:10–22. http://dx.doi.org/10.1038/sj.cdd.4402038.
22. Henry T, Monack DM. 2007. Activation of the inflammasome upon Francisella tularensis infection: interplay of innate immune pathways and virulence factors. Cell Microbiol 9:2543–2551. http://dx.doi.org/10.1111/j.1462-5822.2007.01022.x.
23. Ren T, Zamboni DS, Roy CR, Dietrich WF, Vance RE. 2006. Flagellin-deficient Legionella mutants evade caspase-1- and Naip5-mediated macrophage immunity. PLoS Pathog 2:e18. http://dx.doi.org/10.1371/journal.ppat.0020018.
24. Harder J, Franchi L, Muñoz-Planillo R, Park JH, Reimer T, Núñez G. 2009. Activation of the Nlrp3 inflammasome by Streptococcus pyogenes requires streptolysin O and NF-kappa B activation but proceeds independently of TLR signaling and P2X7 receptor. J Immunol 183:5823–5829. http://dx.doi.org/10.4049/jimmunol.0900444.
25. Kansal RG, McGeer A, Low DE, Norrby-Teglund A, Kotb M. 2000. Inverse relation between disease severity and expression of the streptococcal cysteine protease, SpeB, among clonal M1T1 isolates recovered from invasive group A streptococcal infection cases. Infect Immun 68:6362–6369. http://dx.doi.org/10.1128/IAI.68.11.6362-6369.2000.
26. Aachoui Y, Sagulenko V, Miao EA, Stacey KJ. 2013. Inflammasome-mediated pyroptotic and apoptotic cell death, and defense against infection. Curr Opin Microbiol 16:319–326. http://dx.doi.org/10.1016/j.mib.2013.04.004.
27. Zheng Y, Lilo S, Mena P, Bliska JB. 2012. YopJ-induced caspase-1 activation in Yersinia-infected macrophages: independent of apoptosis, linked to necrosis, dispensable for innate host defense. PLoS One 7:e36019. http://dx.doi.org/10.1371/journal.pone.0036019.
28. Pazyar N, Feily A, Yaghoobi R. 2012. An overview of interleukin-1 receptor antagonist, anakinra, in the treatment of cutaneous diseases.

Curr Clin Pharmacol **7**:271–275. http://dx.doi.org/10.2174/157488412803305821.

29. **Iglewski BH, Liu PV, Kabat D**. 1977. Mechanism of action of Pseudomonas aeruginosa exotoxin A: adenosine diphosphate-ribosylation of mammalian elongation factor 2 in vitro and in vivo. Infect Immun **15**:138–144.

30. **Jenkins CE, Swiatoniowski A, Issekutz AC, Lin TJ**. 2004. Pseudomonas aeruginosa exotoxin A induces human mast cell apoptosis by a caspase-8 and -3-dependent mechanism. J Biol Chem **279**:37201–37207. http://dx.doi.org/10.1074/jbc.M405594200.

31. **Mühlen KA, Schümann J, Wittke F, Stenger S, Van Rooijen N, Van Kaer L, Tiegs G**. 2004. NK cells, but not NKT cells, are involved in Pseudomonas aeruginosa exotoxin A-induced hepatotoxicity in mice. J Immunol **172**:3034–3041. http://dx.doi.org/10.4049/jimmunol.172.5.3034.

32. **Lima-Junior DS, Costa DL, Carregaro V, Cunha LD, Silva AL, Mineo TW, Gutierrez FR, Bellio M, Bortoluci KR, Flavell RA, Bozza MT, Silva JS, Zamboni DS**. 2013. Inflammasome-derived IL-1beta production induces nitric oxide-mediated resistance to Leishmania. Nat Med **19**:909–915. http://dx.doi.org/10.1038/nm.3221.

33. **Dockrell DH, Marriott HM, Prince LR, Ridger VC, Ince PG, Hellewell PG, Whyte MK**. 2003. Alveolar macrophage apoptosis contributes to pneumococcal clearance in a resolving model of pulmonary infection. J Immunol **171**:5380–5388. http://dx.doi.org/10.4049/jimmunol.171.10.5380.

34. **Ali F, Lee ME, Iannelli F, Pozzi G, Mitchell TJ, Read RC, Dockrell DH**. 2003. Streptococcus pneumoniae-associated human macrophage apoptosis after bacterial internalization via complement and Fcgamma receptors correlates with intracellular bacterial load. J Infect Dis **188**:1119–1131. http://dx.doi.org/10.1086/378675.

35. **Kobayashi SD, Braughton KR, Whitney AR, Voyich JM, Schwan TG, Musser JM, DeLeo FR**. 2003. Bacterial pathogens modulate an apoptosis differentiation program in human neutrophils. Proc Natl Acad Sci U S A **100**:10948–10953. http://dx.doi.org/10.1073/pnas.3333375100.

36. **Stecher B, Robbiani R, Walker AW, Westendorf AM, Barthel M, Kremer M, Chaffron S, Macpherson AJ, Buer J, Parkhill J, Dougan G, von Mering C, Hardt WD**. 2007. Salmonella enterica serovar typhimurium exploits inflammation to compete with the intestinal microbiota. PLoS Biol **5**:2177–2189. http://dx.doi.org/10.1371/journal.pbio.0050244.

37. **Winter SE, Thiennimitr P, Winter MG, Butler BP, Huseby DL, Crawford RW, Russell JM, Bevins CL, Adams LG, Tsolis RM, Roth JR, Bäumler AJ**. 2010. Gut inflammation provides a respiratory electron acceptor for salmonella. Nature **467**:426–429. http://dx.doi.org/10.1038/nature09415.

38. **Hruz P, Zinkernagel AS, Jenikova G, Botwin GJ, Hugot JP, Karin M, Nizet V, Eckmann L**. 2009. NOD2 contributes to cutaneous defense against Staphylococcus aureus through alpha-toxin-dependent innate immune activation. Proc Natl Acad Sci U S A **106**:12873–12878. http://dx.doi.org/10.1073/pnas.0904958106.

39. **Ali SR, Timmer AM, Bilgrami S, Park EJ, Eckmann L, Nizet V, Karin M**. 2011. Anthrax toxin induces macrophage death by p38 MAPK inhibition but leads to inflammasome activation via ATP leakage. Immunity **35**:34–44. http://dx.doi.org/10.1016/j.immuni.2011.04.015.

40. **Chang YC, Uchiyama S, Varki A, Nizet V**. 2012. Leukocyte inflammatory responses provoked by pneumococcal sialidase. mBio **3**:e00220-11. http://dx.doi.org/10.1128/mBio.00220-11.

41. **Hollands A, Pence MA, Timmer AM, Osvath SR, Turnbull L, Whitchurch CB, Walker MJ, Nizet V**. 2010. Genetic switch to hypervirulence reduces colonization phenotypes of the globally disseminated group A streptococcus M1T1 clone. J Infect Dis **202**:11–19. http://dx.doi.org/10.1086/653124.

42. **Aziz RK, Pabst MJ, Jeng A, Kansal R, Low DE, Nizet V, Kotb M**. 2004. Invasive M1T1 group A streptococcus undergoes a phase-shift in vivo to prevent proteolytic degradation of multiple virulence factors by SpeB. Mol Microbiol **51**:123–134. http://dx.doi.org/10.1046/j.1365-2958.2003.03797.x.

43. **Hamilton A, Robinson C, Sutcliffe IC, Slater J, Maskell DJ, Davis-Poynter N, Smith K, Waller A, Harrington DJ**. 2006. Mutation of the maturase lipoprotein attenuates the virulence of Streptococcus equi to a greater extent than does loss of general lipoprotein lipidation. Infect Immun **74**:6907–6919. http://dx.doi.org/10.1128/IAI.01116-06.

44. **Kraemer GR, Iandolo JJ**. 1990. High-frequency transformation of Staphylococcus aureus by electroporation. Curr Microbiol **21**:373–376. http://dx.doi.org/10.1007/BF02199440.

45. **Lin AE, Guttman JA**. 2012. The Escherichia coli adherence factor plasmid of enteropathogenic Escherichia coli causes a global decrease in ubiquitylated host cell proteins by decreasing ubiquitin E1 enzyme expression through host aspartyl proteases. Int J Biochem Cell Biol **44**:2223–2232. http://dx.doi.org/10.1016/j.biocel.2012.09.005.

46. **Pfaffl MW**. 2001. A new mathematical model for relative quantification in real-time RT-PCR. Nucleic Acids Res **29**:e45. http://dx.doi.org/10.1093/nar/29.9.e45.

47. **Lin AE, Autran CA, Lin AE, Autran CA, Espanola SD, Bode L, Nizet V**. 2013. Human milk oligosaccharides protect bladder epithelial cells against uropathogenic *Escherichia coli* invasion and cytotoxicity. J Infect Dis **209**:389–398. http://dx.doi.org/10.1093/infdis/jit464.

48. **Timmer AM, Timmer JC, Pence MA, Hsu LC, Ghochani M, Frey TG, Karin M, Salvesen GS, Nizet V**. 2009. Streptolysin O promotes group A streptococcus immune evasion by accelerated macrophage apoptosis. J Biol Chem **284**:862–871. http://dx.doi.org/10.1074/jbc.M804632200.